Comp. Appl. Math.
DOI 10.1007/s40314-014-0133-z

An *hp* finite element adaptive scheme to solve the Poisson problem on curved domains

M. G. Armentano · C. Padra · M. Scheble

Received: 2 October 2013 / Revised: 3 February 2014 / Accepted: 21 March 2014

Abstract In this work, we introduce an *hp* finite element method for two-dimensional Poisson problems on curved domains using curved elements. We obtain a priori error estimates and define a local a posteriori error estimator of residual type. We show, under appropriate assumptions about the curved domain, the global reliability and the local efficiency of the estimator. More precisely, we prove that the estimator is equivalent to the energy norm of the error up to higher-order terms. The equivalence constant of the efficiency estimate depends on the polynomial degree. We also present an *hp* adaptive algorithm and several numerical tests which show the performance of the adaptive strategy.

Keywords Finite elements · *hp* version · Curved domains · A posteriori error estimates

Mathematics Subject Classification 65N30 · 65N15 · 65N50

1 Introduction

The goal of this paper is to introduce and analyze an *hp* finite element scheme for solving the Poisson problem on curved domains using curved elements. This elements are suitable for use along the curved part of the boundary. Adaptive procedures based on a posteriori error estimators play a relevant role in the numerical approximation of partial differential equations. In fact, there are several papers concerning the development of a posteriori error estimates and efficient adaptive schemes for the *h* finite element approximation of a wide range of problems (see, for example, Verfürth 1996 and the references there in).

Communicated by André Nachbin.

M. G. Armentano (✉)
Departamento de Matemática, Facultad de Ciencias Exactas y Naturales, Universidad de Buenos Aires, IMAS-Conicet, 1428 Buenos Aires, Argentina
e-mail: garmenta@dm.uba.ar

C. Padra · M. Scheble
Centro Atómico Bariloche, 4800 Bariloche, Argentina

Published online: 11 April 2014

There are also some references regarding the hp finite element approximation for different type of problems (see, for instance, Armentano et al. 2011; Azaiez et al. 2008; Boffi et al. 2006; Melenk and Wohlmuth 2001; Schwab 1998). However, to the authors' knowledge, all analysis for the hp approach are restricted, in general, to the case of polygonal domains, or by replacing the curved domain Ω with a polygonal domain Ω_h. These approaches, however, do not retain the same accuracy along the curved part of the original boundary. Different approaches have been considered, for instance by Ciarlet and Raviart (1972), Scott (1975) and Zlâmal (1973), to deal with curved domains. In this work, we consider curved element (like those introduced in Zlâmal 1973) that are suitable for the curved part of the boundary of Ω.

On the other hand, a posteriori error analysis for the hp version of the finite element method still presents several difficulties even for source problems in polygonal domains (see, for instance, Ainsworth and Senior 1997, 1998; Melenk and Wohlmuth 2001; Tarancon et al. 2005 and the references therein). One of the main difficulties in hp adaptivity arises from the fact that the accuracy can be improved by subdividing elements or by increasing the polynomial degree. Consequently at each refinement step, it is necessary to decide which of these two options must be chosen. There are different hp adaptive strategies (see, for example, Ainsworth and Senior 1997, 1998; García-Castillo et al. 2007; Demkowicz 2007; Demkowicz et al. 2008; Oden et al. 1995, 1992; Pardo et al. 2007). Some of them follow the strategy developed by Demkowicz (2007), Demkowicz et al. (2008), while others are based on the estimation of the local regularity of the solution. Within the second kind of strategies, we find the one proposed by Melenk and Wohlmuth (2001), based on a predictor of the error in each element of the mesh.

In this work, we obtain a priori error estimates and develop a posteriori error estimator of residual type using curved elements which fit the curved domain. We analyze the equivalence of this estimator with the energy norm of the error. We prove, under appropriate assumptions about the curved domain, the global reliability of the error indicator up to higher-order terms. Moreover, we also show the local efficiency of the indicator with a constant which depends on the polynomial degree of the element. To the best of the authors' knowledge, simultaneous reliability and efficiency estimates with constants independent of the polynomial degree have been obtained only for the one-dimensional case (Dorfler and Heuveline 2007). In fact, in the two-dimensional case, this kind of estimates has not yet been proved for any a posteriori error estimator for hp finite element methods.

Following the hp adaptive strategy given in Armentano et al. (2011, 2012), Melenk and Wohlmuth (2001), we propose an adaptive algorithm and apply it to different curved domains. These numerical tests allow us to show a good performance of the error indicator and the adaptive algorithm.

The rest of the paper is organized as follows. In Sect. 2, we introduce the problem. In Sect. 3, we present the hp finite element approximation and obtain a priori error estimates. In Sect. 4, we introduce a posteriori error estimator and prove its equivalence with the energy norm of the error. Finally, in Sect. 5, we report several numerical examples that allow assessing the performance of the adaptive scheme.

2 The state of the problem

Let $\Omega \subset \mathbb{R}^2$ be a bounded open domain, in general, nonconvex, with a piecewise smooth Lipschitz boundary Γ. We assume that Γ belongs to C^{k+1} piecewise with $k \geq 1$ sufficiently large to fulfill our requirements.

Fig. 1 Curved triangle

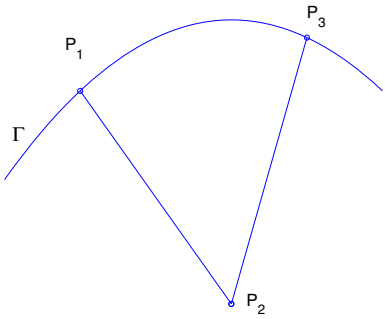

Our model problem is

$$\begin{cases} -\Delta u = f & \text{in } \Omega, \\ u = 0 & \text{on } \Gamma. \end{cases} \tag{1}$$

Let $V = H_0^1(\Omega)$. The weak formulation of problem (1) is to find $u \in V$ such that

$$\int_\Omega \nabla u \cdot \nabla v = \int_\Omega f v \quad \forall v \in V. \tag{2}$$

A natural way to approximate the solution of problem (1) is to replace Ω with a polygonal domain and to use the classical finite element method in its h, p or hp version. In this work, we consider curved element that are suitable for the curved part of Γ.

The domain $\overline{\Omega}$ is subdivided into a finite number of (closed) triangles. We assume that the boundary Γ can be divided into a finite number of arcs. For triangles without edges in Γ, we use standard linear triangles. For triangles T with an edge $\ell \subset \partial T \cap \Gamma$, we use the local numbering $\{P_1, P_2, P_3\}$, where P_2 is in the interior of Ω and $P_1, P_3 \in \Gamma$. Consequently, the arc $\ell = \widehat{P_1 P_3} \subset \Gamma$ (see Fig. 1). We assume that each of those arcs has a parametric representation $(\phi(s), \psi(s))$, $a \le s \le b$, with functions $\phi, \psi \in C^{k+1}([a, b])$.

We denote by h_T and θ_T the greatest side and smallest angle of the triangle of vertices P_1, P_2, P_3, respectively.

Let $\hat{T}$ be the classical reference triangle, i.e., the triangle of vertices $(0, 0)$, $(1, 0)$ and $(0, 1)$. For each triangle T in the triangulation, we introduce an application F which maps the triangle $\hat{T}$ on the triangle T. If we denote by (x_j, y_j), $1 \le j \le 3$, the coordinates of the vertices P_j of T, then the mapping F can be defined as (see Zlâmal 1973):

$$F(\xi, \eta) = F_0(\xi, \eta) + (1 - \xi - \eta)\,(\Phi(\eta), \Psi(\eta)), \tag{3}$$

where F_0 is the affine transformation from $\hat{T}$ onto the triangle of vertices P_1, P_2 and P_3:

$$F_0(\xi, \eta) = (x_1 + (x_2 - x_1)\xi + (x_3 - x_1)\eta,\, y_1 + (y_2 - y_1)\xi + (y_3 - y_1)\eta).$$

Functions Φ and Ψ are defined as:

$$\Phi(\eta) = \frac{\phi(s_1 + (s_3 - s_1)\eta) - x_1 - (x_3 - x_1)\eta}{1 - \eta},$$

$$\Psi(\eta) = \frac{\psi(s_1 + (s_3 - s_1)\eta) - y_1 - (y_3 - y_1)\eta}{1 - \eta},$$

with s_1 and s_3, the values of the parameters corresponding to the vertices P_1 and P_3, respectively. We remark that the point $\eta = 1$ is only an apparent singularity. Indeed, it is possible to extend $\Phi(\eta)$ and $\Psi(\eta)$ for $\eta = 1$ such that they belong to C^k (see Zlâmal 1973).

Then, given a polynomial function $\hat{v}(\xi, \eta)$ in $\hat{T}$ with degree p, we can define a function $v(x, y)$ in T by $v(x, y) = \hat{v}(F^{-1}(x, y))$. We say that v has "degree" $p_T = p$ in T.

The next theorem presents some properties of transformation F. Although the result is a particular case of Theorem 1 in Zlâmal (1973), we include it for the sake of completeness.

Theorem 1 *Let Γ be of class C^{k+1} piecewise with $k \geq 1$. If h is sufficiently small, the transformation F maps $\hat{T}$ one-to-one on T. The Jacobian $J_F(\xi, \eta)$ of this mapping is different from zero on $\hat{T}$, the side $\overline{(0,0)(0,1)}$ is mapped on the arc $\widehat{P_1P_3}$, the sides $\overline{(0.0)(1,0)}$ and $\overline{(1,0)(0,1)}$ are linearly mapped on the sides $\overline{P_1P_2}$ and $\overline{P_2P_3}$, respectively. The mapping and its inverse mapping are of class C^k. In addition,*

$$|J_F(\xi, \eta)| = O(h_T^2), \tag{4}$$

$$D^j F_i(\xi, \eta) = O(h_T^{|j|}) \quad 1 \leq |j| \leq k, \tag{5}$$

$$D^j F_i^{-1}(\xi, \eta) = O(h_T^{-1}) \quad |j| = 1, \tag{6}$$

where $j = (j_1, j_2)$, $|j| = j_1 + j_2$ and $D^j F_i(\xi, \eta) = \dfrac{\partial^{|j|} F_i}{\partial \xi^{j_1} \partial \eta^{j_2}}$.

3 The *hp* finite element approximation and a priori error estimates

In this section, we introduce an hp finite element method for the Poisson problem described in the previous section, prove its convergence and obtain a priori error estimates.

Let $\{\mathcal{T}_h\}$ be a family of triangulations of Ω such that any two triangles in $\mathcal{T}_h$ share at most a vertex or an edge. We assume that the family of triangulations $\{\mathcal{T}_h\}$ satisfies a minimum angle condition, i.e., there exists a constant $\theta_0 > 0$ such that $\theta_T \geq \theta_0$, for any $T \in \mathcal{T}_h$.

We associate with each element $T \in \mathcal{T}_h$ a (maximal) polynomial degree $p_T \in \mathbb{N}$. We assume that the polynomial degrees of neighboring elements are comparable, i.e., there exists a constant $\gamma > 0$ such that

$$\gamma^{-1} p_T \leq p_{T'} \leq \gamma p_T \qquad \forall T,\ T' \in \mathcal{T}_h \text{ with } T \cap T' \neq \emptyset. \tag{7}$$

We denote $\boldsymbol{p} := \{p_T\}_{T \in \mathcal{T}_h}$ the family of polynomial degrees.

Throughout the work, we denote by C a generic positive constant (not necessarily the same at each occurrence), which may depend on the mesh and the degree of the polynomials only through the parameters θ_0 and γ, respectively.

We define the finite element space as follows:

$$V_h^{\boldsymbol{p}} := \left\{ v \in V : \ v|_T = \hat{v} \circ F^{-1}, \quad \hat{v} \in \mathcal{P}_{p_T} \ \forall T \in \mathcal{T}_h \right\},$$

where $\mathcal{P}_k$ denotes the space of polynomials of degree at most k.

The discrete problem associated with (1) is to find $u_h \in V_h^{\boldsymbol{p}}$ such that

$$\int_\Omega \nabla u_h \cdot \nabla v = \int_\Omega f v \qquad \forall v \in V_h^{\boldsymbol{p}}. \tag{8}$$

The norms and seminorms in $H^m(D)$, with m an integer, and the norm in $L^\infty(D)$ are denoted by $\|\cdot\|_{m,D}$, $|\cdot|_{m,D}$ and $|\cdot|_{\infty,D}$, respectively. The inner product in $L^2(D)$ for any subdomain $D \subset \Omega$ is denoted by $(\cdot, \cdot)_D$. The domain subscript is dropped for the case $D = \Omega$.

As a consequence of the classical a priori estimates (see Grisvard 1985), the solution of (2) is known to satisfy some further regularity for any $f \in L^2(\Omega)$. In fact, $u \in H^{1+r}(\Omega)$ for some $r > 0$ depending on the geometry of Ω and it holds

$$\|u\|_{1+r} \leq C\|f\|_2, \tag{9}$$

with $r = 1$, when Ω is an smooth domain [see Grisvard 1985, Theorem 2.2.2.3 and (2.3.1.1)] or is a polygonal domain without reentrant corners. In the particular case in which Ω is a polygonal domain with reentrant corners, we have $r < \frac{2\pi}{\theta}$ with θ being the largest interior angle of Ω.

Our first goal is to prove that the solutions of the discrete problem (8) converge to the solution of problem (1). To do this, we present the following Lemma that is a particular case of Theorem 4.3.2 of Ciarlet (1978).

Lemma 1 *If $\hat{v} : \hat{T} \to \mathbb{R}$ is a function in $H^k(\hat{T})$, for some $k \in \mathbb{Z}_{\geq 0}$, the function $v = \hat{v} \circ F^{-1} : T \to \mathbb{R}$ belongs to $H^k(T)$ and there exists a constant C such that*

$$|v|_{0,T} \leq |J_F|^{1/2}_{\infty,\hat{T}} |\hat{v}|_{0,\hat{T}}, \quad \forall \hat{v} \in L^2(\hat{T}), \tag{10}$$

$$|v|_{1,T} \leq C|J_F|^{1/2}_{\infty,\hat{T}} |DF^{-1}|_{\infty,T} |\hat{v}|_{1,\hat{T}}, \quad \forall \hat{v} \in H^1(\hat{T}), \tag{11}$$

$$|v|_{2,T} \leq C|J_F|^{1/2}_{\infty,\hat{T}} \left(|DF^{-1}|^2_{\infty,T} |\hat{v}|_{2,\hat{T}} + |D^2F^{-1}|_{\infty,T} |\hat{v}|_{1,\hat{T}} \right), \quad \forall \hat{v} \in H^2(\hat{T}). \tag{12}$$

Now, we are in a position to prove the following a priori error estimates.

Proposition 1 *For all $r < \frac{\pi}{\theta}$, there exist positive constants C and κ, such that, if $\max_{T \in \mathscr{T}_h} \frac{h_T}{p_T} < \kappa$, then*

$$|u - u_h|_1 \leq C \left(\max_{T \in \mathscr{T}_h} \frac{h_T}{p_T} \right)^r. \tag{13}$$

Proof It can be seen from Babuška and Suri (1994, Theorem 4.1), Babuška and Suri (1987, Lemma 4.5, Theorem 4.6), Oden et al. (1989, Theorem 2.1) and standard results on interpolation in Sobolev spaces (see, for instance, Theorem 1.4 in Girault and Raviart 1986) that there exists an operator $\Pi_h^{\boldsymbol{p}}$ satisfying

$$\|\hat{v} - \Pi_h^{\boldsymbol{p}} \hat{v}\|^2_{1,\hat{T}} \leq C \left(\frac{1}{p'_{\hat{T}}} \right)^{2r} \|\hat{v}\|^2_{1+r,\hat{T}}$$

for any function $\hat{v} \in H^{1+r}(\hat{T})$. Then, the estimate (13) is a direct consequence of a simple changes of variables, Theorem 1, Lemma 1, the fact that $\sum_{T \in \mathscr{T}_h} \|v\|^2_{1+r,T} \leq C\|v\|^2_{1+r}$ and the a priori estimate (9). □

4 A posteriori error estimator

In this section, we present a posteriori error estimator for the error $e := u - u_h$ in the energy norm. We show global reliability and local efficiency by proving that the estimator is equivalent to the energy norm of the error up to higher-order terms. The equivalence constant of the efficiency estimate is suboptimal in that it depends on the polynomial degree.

We introduce here some notation that we use in the definition and analysis of the error estimator. For any $T \in \mathscr{T}_h$, let $\mathscr{E}_T$ denote the set of edges of T and $\mathscr{E} := \bigcup_{T \in \mathscr{T}_h} \mathscr{E}_T$. We decompose $\mathscr{E}$ in disjoint sets $\mathscr{E}_\Gamma := \{\ell \in \mathscr{E} : \ell \subset \Gamma\}$, and $\mathscr{E}_\Omega := \mathscr{E} \setminus \mathscr{E}_\Gamma$.

For each $\ell \in \mathscr{E}_\Omega$, we choose a unit normal vector $\boldsymbol{n}_\ell$ and denote the two triangles sharing this edge T_{in} and T_{out}, with $\boldsymbol{n}_\ell$ pointing outwards T_{in}. For $v_h \in V_h^{\boldsymbol{p}}$, we set

$$\left[\!\left[\frac{\partial v_h}{\partial n} \right]\!\right]_\ell := \nabla \left(v_h|_{T_{\text{out}}} \right) \cdot \boldsymbol{n}_\ell - \nabla \left(v_h|_{T_{\text{in}}} \right) \cdot \boldsymbol{n}_\ell,$$

which corresponds to the jump of the normal derivative of v_h across the edge ℓ. Notice that this value is independent of the chosen direction of the normal vector $\boldsymbol{n}_\ell$.

From (2) and (8), we know that for any $v_h \in V_h^{\boldsymbol{p}}$, the error e satisfies

$$\int_\Omega \nabla e \cdot \nabla v_h = 0. \tag{14}$$

On the other hand, for any $v \in V$, using (2) and integrating by parts, we obtain

$$\int_\Omega \nabla e \cdot \nabla v = \sum_{T \in \mathscr{T}_h} \int_T (f + \Delta u_h) v + \sum_{T \in \mathscr{T}_h} \int_{\partial T} \frac{\partial u_h}{\partial n} v.$$

Hence, defining for each edge $\ell \in \mathscr{E}_\Omega$

$$J_\ell := \frac{1}{2} \left[\!\left[\frac{\partial u_h}{\partial n} \right]\!\right]_\ell,$$

we have

$$\int_\Omega \nabla e \cdot \nabla v = \sum_{T \in \mathscr{T}_h} \left(\int_T (f + \Delta u_h) v + \sum_{\ell \in \mathscr{E}_T} \int_\ell J_\ell v \right) \tag{15}$$

for all $v \in V$.

Let $P_h^{\boldsymbol{p}}$ denote the L^2 projection onto $V_h^{\boldsymbol{p}}$ defined for any $f \in L^2(\Omega)$ by

$$P_h^{\boldsymbol{p}} f \in V_h^{\boldsymbol{p}} : \qquad \int_\Omega P_h^{\boldsymbol{p}} f v_h = \int_\Omega f v_h \qquad \forall v_h \in V_h^{\boldsymbol{p}}. \tag{16}$$

For each element $T \in \mathscr{T}_h$, we define the local error indicator η_T by

$$\eta_T^2 := \frac{h_T^2}{p_T^2} \left\| P_h^{\boldsymbol{p}} f + \Delta u_h \right\|_{0,T}^2 + \sum_{\ell \in \mathscr{E}_T} \frac{|\ell|}{p_\ell} \left\| J_\ell \right\|_{0,\ell}^2, \tag{17}$$

with $p_\ell := \max \{ p_T : \ \ell \in \mathscr{E}_T \}$ and the global error estimator η_Ω by

$$\eta_\Omega^2 := \sum_{T \in \mathscr{T}_h} \eta_T^2.$$

To compare the error and the estimator, we need some interpolation error estimates similar to the hp Clément interpolation operator (see, for example, Melenk and Wohlmuth 2001), valid for standard triangulation.

We introduced the following notation: for each vertex, V of the triangulation $\mathscr{T}_h$,

$$\begin{aligned}
\omega_V &:= \bigcup \{ T \in \mathscr{T}_h : \ V \text{ is a vertex of } T \}, \\
\omega_T &:= \bigcup \{ \omega_V : \ V \text{ is a vertex of } T \}, \\
\omega_L &:= \bigcup \{ \omega_V : \ V \text{ is an endpoint of } \ell \}, \\
\mathscr{E}_V &:= \{ \ell \in \mathscr{E} : V \text{ is an endpoint of } \ell \}.
\end{aligned}$$

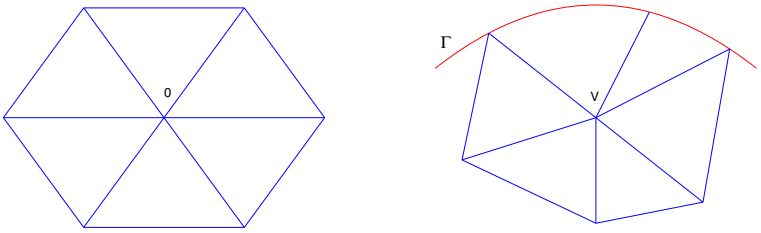

Fig. 2 patches $\widehat{\omega_V}$ and ω_V

The next step in our construction consists in associating any patch ω_V with a reference patch $\widehat{\omega_V}$. If N_V denotes the number of triangles in ω_V, then the corresponding reference patch $\widehat{\omega_V}$ is the regular polygon with N_V edges of length 1 centered at the origin 0, triangulated with N_V triangles all sharing the vertex 0 (see Fig. 2). The patch ω_V can be related to the reference patch by a homeomorphism $F_V : \widehat{\omega_V} \to \omega_V$ with $F_V(0) = V$ which has the form

$$F_V|_T := F \circ F_A^{-1},$$

where the maps F_A are the affine transformation between $\hat{T}$ and the triangles in $\widehat{\omega_V}$ Melenk (2005). Now, we are in condition to obtain the following interpolation error estimates

Lemma 2 *There exists a bounded linear operator $I_h^{\boldsymbol{p}} : V \to V_h^{\boldsymbol{p}}$ such that for any $T \in \mathscr{T}_h$ and for all edges $\ell \in \mathscr{E}$*

$$\left\|u - I_h^{\boldsymbol{p}} u\right\|_{0,T} + \frac{h_T}{p_T}\left\|\nabla(u - I_h^{\boldsymbol{p}} u)\right\|_{0,T} \leq C\frac{h_T}{p_T}|u|_{1,\omega_T}, \tag{18}$$

$$\left\|u - I_h^{\boldsymbol{p}} u\right\|_{0,\ell} \leq C\left(\frac{h_\ell}{p_\ell}\right)^{\frac{1}{2}}|u|_{1,\omega_L}. \tag{19}$$

Proof Following the ideas given above, for each triangulation $\mathscr{T}_h$, we can associated a reference triangulation $\widehat{\mathscr{T}_h}$ by connecting, for all $v \in \mathscr{E}$, patches like $\widehat{\omega_V}$ with corresponding patches ω_V. Then, for the triangulation $\widehat{\mathscr{T}_h}$ and any function $\hat{u} \in H^1(\widehat{\mathscr{T}_h})$, we can consider $\widehat{I_h^{\boldsymbol{p}}} : \hat{V} \to \widehat{V_h^{\boldsymbol{p}}}$, the well-known hp Clément interpolant, which satisfies (see Melenk 2005):

$$\left\|\hat{u} - \widehat{I_h^{\boldsymbol{p}}}\hat{u}\right\|_{0,\hat{T}} + \frac{1}{p_T}\left\|\nabla(\hat{u} - \widehat{I_h^{\boldsymbol{p}}}\hat{u})\right\|_{0,\hat{T}} \leq C\frac{1}{p_T}|\hat{u}|_{1,\widehat{\omega_T}} \qquad \forall \hat{T} \in \widehat{\mathscr{T}_h}, \tag{20}$$

$$\left\|\hat{u} - \widehat{I_h^{\boldsymbol{p}}}u\right\|_{0,\hat{\ell}} \leq C\left(\frac{1}{p_\ell}\right)^{\frac{1}{2}}|\hat{u}|_{1,\widehat{\omega_L}}, \tag{21}$$

where $\hat{V} = \{v \in H^1(\widehat{\mathscr{T}_h}) : v = 0 \text{ on } \partial\widehat{\mathscr{T}_h}\}$ and $\widehat{V_h^{\boldsymbol{p}}} := \left\{\hat{v} \in \hat{V} : \ \hat{v}\big|_T \in \mathscr{P}_{p_T}\ \forall T \in \widehat{\mathscr{T}_h}\right\}$.

We define the interpolant $I_h^{\boldsymbol{p}}$ as: $I_h^{\boldsymbol{p}}|_{\omega_V} = \widehat{I_h^{\boldsymbol{p}}}|_{\widehat{\omega_V}} \circ F_V$. Then, from Theorem 1 and Lemma 1, the fact that $\|DF_A^{-1}\|_{\infty,\hat{T}} \leq C$ and inequalities (20) and (21), we conclude that

$$\begin{aligned}\left\|u - I_h^{\boldsymbol{p}} u\right\|_{0,T} + \frac{h_T}{p_T}\left\|\nabla(u - I_h^{\boldsymbol{p}} u)\right\|_{0,T} &\leq Ch_T\left(\left\|\hat{u} - \widehat{I_h^{\boldsymbol{p}}}\hat{u}\right\|_{0,\hat{T}} + \frac{1}{p_T}\left\|\nabla(\hat{u} - \widehat{I_h^{\boldsymbol{p}}}\hat{u})\right\|_{0,\hat{T}}\right)\\ &\leq C\frac{h_T}{p_T}|\hat{u}|_{1,\widehat{\omega_T}} \leq C\frac{h_T}{p_T}\sum_{T\subset\widehat{\omega_T}}|\hat{u}|_{1,T}\\ &\leq C\frac{h_T}{p_T}\sum_{T\subset\omega_T}|u|_{1,T} \leq C\frac{h_T}{p_T}|u|_{1,\omega_T}.\end{aligned}$$

The other inequality can be obtained in a similar way. □

The following theorem provides an upper bound for the error, which proves the reliability of the error estimator up to higher-order terms.

Theorem 2 *There exists a positive constant C such that*

$$|e|_1 \leq C \left[\eta_\Omega + \left(\max_{T \in \mathscr{T}_h} \frac{h_T}{p_T} \right) \| f - P_h^{\mathbf{p}} f \|_0 \right]$$

Proof Using the error equations (14) with $v_h = I_h^{\mathbf{p}} e$ and (15) with $v = e - I_h^{\mathbf{p}} e$, we obtain

$$|e|_1^2 = \int_\Omega \nabla e \cdot \nabla \left(e - I_h^{\mathbf{p}} e \right) = \sum_{T \in \mathscr{T}_h} \left(\int_T (f + \Delta u_h) \left(e - I_h^{\mathbf{p}} e \right) + \sum_{\ell \in \mathscr{E}_T} \int_\ell J_\ell (e - I_h^{\mathbf{p}} e) \right)$$

$$= \sum_{T \in \mathscr{T}_h} \left(\int_T (P_h^{\mathbf{p}} f + \Delta u_h) \left(e - I_h^{\mathbf{p}} e \right) + \sum_{\ell \in \mathscr{E}_T} \int_\ell J_\ell (e - I_h^{\mathbf{p}} e) + \int_T (f - P_h^{\mathbf{p}} f)(e - I_h^{\mathbf{p}} e) \right)$$

Then, the result follows using the Cauchy-Schwartz inequality, Lemma 2, the definition of η_Ω and the fact that the triangulation satisfies the minimum angle condition and (7). □

For $T \in \mathscr{T}_h$, let

$$b_T(x, y) := \begin{cases} \hat{b}_T(F^{-1}(x, y)) & \text{in } T, \\ 0 & \text{in } \Omega \setminus T, \end{cases}$$

where $\hat{b}_T$ is the standard cubic bubble given by $\hat{b}_T := \lambda_1 \lambda_2 \lambda_3$, where λ_1, λ_2 and λ_3 denote the barycentric coordinates of $\hat{T}$.

For $\ell \in \mathscr{E}_\Omega$, we denote by T_1 and T_2 the two triangles sharing ℓ and we enumerate the vertices of T_1 and T_2 so that the vertices of ℓ are numbered first. Then, associated with $\omega_\ell = T_1 \cup T_2$, we can define a transformation $F_\ell : \hat{D} \to \omega_\ell$, where $\hat{D} = \hat{T}_1 \cup \hat{T}_2$ with $\hat{T}_1 = \hat{T}$ and $\hat{T}_2$ is the triangle of vertices $(0, 0)$, $(1, 0)$, $(0, -1)$. The bubble function associated with ℓ is defined as:

$$b_\ell(x, y) := \begin{cases} \hat{b}_\ell(F_\ell^{-1}(x, y)) & \text{in } \omega_\ell, \\ 0 & \text{in } \Omega \setminus \omega_\ell, \end{cases}$$

where $\hat{b}_\ell$ is the piecewise quadratic edge bubble function defined by $\hat{b}_\ell := \lambda_1^{\hat{T}_1} \lambda_2^{\hat{T}_2}$.

To guarantee that the error indicator is efficient to guide an adaptive refinement scheme, we should prove that η_T is bounded by the H^1 norm of the error on a neighborhood of T up to higher-order terms. This kind of estimates is in general based on the use of inverse inequalities which hold in piecewise polynomial spaces (see, for example, Ciarlet (1978, pag.140) for the h version of the finite element method and Melenk and Wohlmuth (2001) for the hp version). Next Lemma shows some inverse inequalities for functions in $V_h^{\mathbf{p}}$.

Lemma 3 *For any $v \in V_h^{\mathbf{p}}$ we have that*

$$|v|_{1,T} \leq C \frac{p_T^2}{h_T} \|v\|_{0,T} \qquad \forall T \in \mathscr{T}_h \tag{22}$$

$$|v|_{0,T} \leq C p_T \| v b_T^{\frac{1}{2}} \|_{0,T} \qquad \forall T \in \mathscr{T}_h. \tag{23}$$

Moreover, if $v = 0$ in ∂T, then

$$|v|_{1,T} \leq C \frac{p_T}{h_T} \| \frac{v}{b_T^{\frac{1}{2}}} \|_{0,T} \qquad \forall T \in \mathscr{T}_h. \tag{24}$$

Proof Given $v \in V_h^{\mathbf{p}}$, for any $T \in \mathscr{T}_h$, we know that $v(x, y) = v(F(\xi, \eta)) = \hat{v}(\xi, \eta)$. Then, from Lemma 1 and the inequality (23) in Melenk and Wohlmuth (2001), we obtain

$$|v|_{1,T} \leq C |J_F|_{\infty,\hat{T}}^{1/2} |DF^{-1}|_{\infty,T} |\hat{v}|_{1,\hat{T}} \leq C p_T^2 |J_F|_{\infty,\hat{T}}^{1/2} |DF^{-1}|_{\infty,T} \|\hat{v}\|_{0,\hat{T}} \tag{25}$$

$$\leq C p_T^2 |J_F|_{\infty,\hat{T}}^{1/2} |DF^{-1}|_{\infty,T} |J_{F^{-1}}|_{\infty,T}^{1/2} \|v\|_{0,T}. \tag{26}$$

Now, Theorem 1 provides the first estimate. Analogously, inequalities (23) and (24) are obtained using estimates (22) and (24) in Melenk and Wohlmuth (2001), respectively. □

The following lemma provides an upper estimate for the first term in the definition of η_T [cf. (17)].

Lemma 4 *There exists a positive constant C_{p_T} such that*

$$\frac{h_T}{p_T} \left\| P_h^{\mathbf{p}} f + \Delta u_h \right\|_{0,T} \leq \frac{C_{p_T}}{p_T} \left(C_{p_T} |e|_{1,T} + h_T \| P_h^{\mathbf{p}} f - f \|_{0,T} \right). \tag{27}$$

Proof Using (15) with $v = (P_h^{\mathbf{p}} f + \Delta u_h) b_T \in H_0^1(T) \subset V$, we obtain

$$\int_T \left(P_h^{\mathbf{p}} f + \Delta u_h \right)^2 b_T = \int_T (P_h^{\mathbf{p}} f - f)(P_h^{\mathbf{p}} f + \Delta u_h) b_T + \int_T \nabla e \cdot \nabla \left((P_h^{\mathbf{p}} f + \Delta u_h) b_T \right)$$

$$\leq \| P_h^{\mathbf{p}} f - f \|_{0,T} \| (P_h^{\mathbf{p}} f + \Delta u_h) b_T \|_{0,T} + |e|_{1,T} \, |(P_h^{\mathbf{p}} f + \Delta u_h) b_T|_{1,T}.$$

Since $(P_h^{\mathbf{p}} f + \Delta u_h) b_T \in W_p$, where W_p is a subspace of V with $\dim(W_p) < \infty$, for the same arguments of Lemma 3, we can infer that there exists a constant C_{p_T} such that:

$$|(P_h^{\mathbf{p}} f + \Delta u_h) b_T|_{1,T} \leq \frac{C_{p_T}}{h_T} \| (P_h^{\mathbf{p}} f + \Delta u_h) b_T^{\frac{1}{2}} \|_{0,T},$$

$$\| P_h^{\mathbf{p}} f + \Delta u_h \|_{0,T} \leq C_{p_T} \| (P_h^{\mathbf{p}} f + \Delta u_h) b_T^{\frac{1}{2}} \|_{0,T}.$$

Therefore, we obtain

$$\left\| P_h^{\mathbf{p}} f + \Delta u_h \right\|_{0,T} \leq C_{p_T} \left[\int_T \left(P_h^{\mathbf{p}} f + \Delta u_h \right)^2 b_T \right]^{1/2} \leq C_{p_T} \| P_h^{\mathbf{p}} f - f \|_{0,T} + \frac{C_{p_T}^2}{h_T} |e|_{1,T},$$

and the proof concludes. □

Remark 1 We observe that, in the particular case in which

$$(P_h^{\mathbf{p}} f + \Delta u_h) b_{T|T}(x, y) = (g \circ F^{-1})(x, y) = g(\xi, \eta),$$

for some $g \in \mathscr{P}_{p_T+3}$, from Lemma 3, we have that $C_{p_T} = p_T$.

Next, we prove an upper estimate for the second term in the definition of η_T [cf. (17)].

Lemma 5 *For all $\delta > 0$, there exists a positive constant C_δ such that, if $\ell \in \mathscr{E}_\Omega$, then*

$$\frac{|\ell|^{1/2}}{p_\ell^{1/2}} \|J_\ell\|_{0,\ell} \leq C_\delta p_\ell^{1+\delta} \left[\left(\frac{C_{p_T}}{p_\ell} \right)^2 |e|_{1,\omega_\ell} + \frac{|\ell| C_{p_T}}{p_\ell^2} \|P_h^{\mathbf{p}} f - f\|_{0,\omega_\ell} \right] \tag{28}$$

where $\omega_\ell := \bigcup \{T \in \mathscr{T}_h : \ell \in \mathscr{E}_T\}$.

Proof We follow the arguments proposed in Armentano et al. (2011), Melenk and Wohlmuth (2001). According to Lemma 2.4 from reference Melenk and Wohlmuth (2001) and Eq. (27) from reference Armentano et al. (2011), we know that for all $\beta > 0$, there exists $C_\beta > 0$, depending only on β, such that

$$\|J_\ell\|_{0,\omega_\ell} \leq C_\beta p_\ell^\beta \left(\int_\ell b_\ell^\beta J_\ell^2 \right)^{1/2}. \tag{29}$$

Moreover, using equations (29), (30) from reference Armentano et al. (2011), we have that for all $\beta > \frac{1}{2}$, there exists another constant $C_\beta > 0$ (depending only on β), such that for all $\epsilon > 0$ there exists $v_\epsilon \in H_0^1(\omega_\ell)$ satisfying

$$v_\epsilon|_\ell = b_\ell^\beta J_\ell, \tag{30}$$

$$\|v_\epsilon\|_{0,\omega_\ell}^2 \leq C_\beta \epsilon |\ell| \int_\ell b_\ell^\beta J_\ell^2, \tag{31}$$

$$|v_\epsilon|_{1,\omega_\ell}^2 \leq C_\beta \left[\epsilon p_\ell^{2(2-\beta)} + \epsilon^{-1} \right] \frac{1}{|\ell|} \int_\ell b_\ell^\beta J_\ell^2. \tag{32}$$

In what follows, we denote by C_β a generic positive constant, not necessarily the same at each occurrence, which depends only on β.

For $\ell \in \mathscr{E}_\Omega$, we use (15) with $v = v_\epsilon$ to write

$$\int_{\omega_\ell} \nabla e \cdot \nabla v_\epsilon = \int_{\omega_\ell} (f + \Delta u_h) v_\epsilon + \int_\ell J_\ell v_\epsilon.$$

Hence, using (30), (32), (31) and (27) and Lemma 4, we obtain

$$\begin{aligned}
\int_\ell b_\ell^\beta J_\ell^2 &= \int_\ell J_\ell v_\epsilon \\
&\leq |e|_{1,\omega_\ell} |v_\epsilon|_{1,\omega_\ell} + \left(\|P_h^{\mathbf{p}} f + \Delta u_h\|_{0,\omega_\ell} + \|P_h^{\mathbf{p}} f - f\|_{0,\omega_\ell} \right) \|v_\epsilon\|_{0,\omega_\ell} \\
&\leq \frac{C_\beta}{|\ell|^{1/2}} \left\{ \left[\epsilon p_\ell^{2(2-\beta)} + \epsilon^{-1} + \epsilon C_{p_T}^4 \right]^{1/2} |e|_{1,\omega_\ell} + \epsilon^{\frac{1}{2}} |\ell| C_{p_T} \|P_h^{\mathbf{p}} f - f\|_{0,\omega_\ell} \right\} \left(\int_\ell b_\ell^\beta J_\ell^2 \right)^{1/2}.
\end{aligned}$$

Choosing $\epsilon = p_\ell^{-2}$ in this estimate, we have

$$\left(\int_\ell b_\ell^\beta J_\ell^2 \right)^{1/2} \leq \frac{C_\beta}{|\ell|^{1/2}} \left\{ [p_\ell + \frac{C_{p_T}^2}{p_\ell}] |e|_{1,\omega_\ell} + |\ell| \frac{C_{p_T}}{p_\ell} \|P_h^{\mathbf{p}} f - f\|_{0,\omega_\ell} \right\},$$

from which, taking $\beta = \frac{1}{2} + \delta$ and using (29), we obtain (28). Thus, we conclude the proof. □

Now, we conclude the efficiency of the error indicator, with a constant depending on the polynomial degree.

Theorem 3 *For all $\delta > 0$, there exists a positive constant C_δ such that for all $T \in \mathscr{T}_h$, we get*

$$\eta_T \leq C_\delta p_T^{1+\delta} \left[\left(\frac{C_{p_T}}{p_T} \right)^4 |e|_{1,\Omega_T} + h_T \frac{C_{p_T}}{p_T^2} \| P_h^{\mathbf{p}} f - f \|_{0,\Omega_T} \right],$$

where $\Omega_T := \bigcup \{ T' : T \text{ and } T' \text{ share an edge} \}$.

Proof It is an immediate consequence of Lemmas 4 and 5 and the assumption (7). □

Remark 2 We observe again that, in the particular case in which

$$(P_h^{\mathbf{p}} f + \Delta u_h) b_{T\,|T}(x, y) = (g \circ F^{-1})(x, y) = g(\xi, \eta),$$

for some $g \in \mathscr{P}_{p_T+3}$, from Lemma 3, we have that $C_{p_T} = p_T$ and so in this case, we can conclude that: for all $\delta > 0$, there exists a positive constant C_δ such that for all $T \in \mathscr{T}_h$,

$$\eta_T \leq C_\delta p_T^{1+\delta} \left[|e|_{1,\Omega_T} + \frac{h_T}{p_T} \| P_h^{\mathbf{p}} f - f \|_{0,\Omega_T} \right].$$

Remark 3 In the case of polygonal domains from (3), we have that $F \equiv F_0$ and therefore the estimates of Remarks 1 and 2 agree with the standard results of Melenk and Wohlmuth (2001).

4.1 Adaptive refinement strategy

In this section, we present the adaptive refinement strategy that is the same used in Armentano et al. (2011, 2012), Melenk and Wohlmuth (2001). Indeed, to determine which elements should be refined, we use the mean value strategy: all the triangles $T \in \mathscr{T}_h$ with $\eta_T \geq \theta \eta_{\mathrm{M}}$ are marked to be refined, where

$$\eta_{\mathrm{M}}^2 := \frac{1}{\#\mathscr{T}_h} \sum_{T \in \mathscr{T}_h} \eta_T^2.$$

Here, $\theta \in (0, 1)$ is a parameter which can be arbitrarily chosen with the additional consideration that at each step, for each marked triangle, it has to be decided whether to perform a p refinement or an h refinement.

In the case of p refinement, the degree p_T of the marked element is increased by one and the triangle is kept fixed. While in the case of h refinement, the marked element T is subdivided into four triangles: $T = \bigcup_{j=1}^4 T_j'$. We assign to the new elements T_j' the same degree of T: $p_{T_j'} = p_T$. The conformity of the mesh is preserved by means of a longest edge subdivision strategy on the unrefined neighboring triangles (see Verfürth 1996).

In order to decide whether to apply a p or an h refinement to a particular triangle, we follow the approach proposed in Melenk and Wohlmuth (2001), which is based on the comparison of the current local estimated error with a prediction of this error obtained from the preceding step. If at the preceding step there was an h refinement leading to $T = \bigcup_{j=1}^k T_j'$, $k = 2, 3, 4$, then the prediction indicator is defined as follows:

$$\left(\eta_{T_j'}^{\mathrm{pred}} \right)^2 := \gamma_h \left(\frac{|T_j'|}{|T|} \right)^{p_T+1} \eta_T^2,$$

Table 1 Refinement algorithm

If $\eta_T^2 \geq \theta \eta_M^2$ then
  if $\eta_T^2 \geq \left(\eta_T^{\text{pred}}\right)^2$ then
    subdivide T into 4 triangles T'_j, $1 \leq j \leq 4$
    longest edge strategy to maintain mesh conformity
    $p_{T'_j} := p_T$
    $\left(\eta_{T'_j}^{\text{pred}}\right)^2 := \gamma_h \left(\frac{|T'_j|}{|T|}\right)^{p_T+1} \eta_T^2$
  else
    $p_T := p_T + 1$
    $\left(\eta_T^{\text{pred}}\right)^2 := \gamma_p \eta_T^2$
  end
else
  $\left(\eta_T^{\text{pred}}\right)^2 := \gamma_n \left(\eta_T^{\text{pred}}\right)^2$
end

where γ_h is a control parameter to be determined. On the other hand, if at the preceding step there was a p refinement on the element T, then the prediction indicator is defined by

$$\left(\eta_T^{\text{pred}}\right)^2 := \gamma_p \eta_T^2,$$

where $\gamma_p \in (0, 1)$ is a reduction factor which is chosen arbitrarily. Finally, for elements, neither p nor h refined at the preceding step:

$$\left(\eta_T^{\text{pred}}\right)^2 := \gamma_n \left(\eta_T^{\text{pred}}\right)^2,$$

where γ_n is a reduction or amplification factor also arbitrarily chosen. In all cases, we proceed to an h refinement of T when the error indicator η_T is larger than the prediction indicator η_T^{pred} and to a p refinement otherwise.

Altogether, we arrive at the algorithm shown in Table 1.

We set $\eta_T^{\text{pred}} := 0$ for all elements T on the initial triangulation, so that the first step is a purely h refinement on all elements.

5 Numerical examples

In this section, we present some numerical results that allow us to assess the performance of the proposed hp-adaptive scheme on curved domains. We present three examples. In the first one, a problem with available regular solution is considered. The algorithm is also applied without using curvilinear elements to exhibit the loss of convergence rate. A similar analysis is performed in the second example, but for this case, the solution has a singularity due to the presence of a reentrant vertex in the domain. In the third example, the algorithm is used to solve a problem of practical interest on a rather complex domain.

The color palette used in the figures indicates the polynomial degree of each element.

5.1 Test 1: Annular domain

In this first test, we have considered an annular domain centered in the origin with inner radius $r_i = 0.5$ and outer radius $r_o = 1$. The domain and the initial mesh with linear finite

Fig. 3 Domain and initial mesh

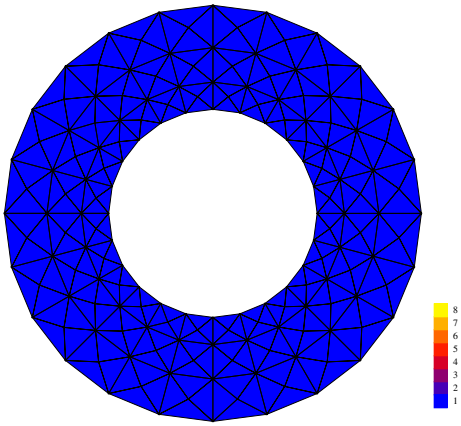

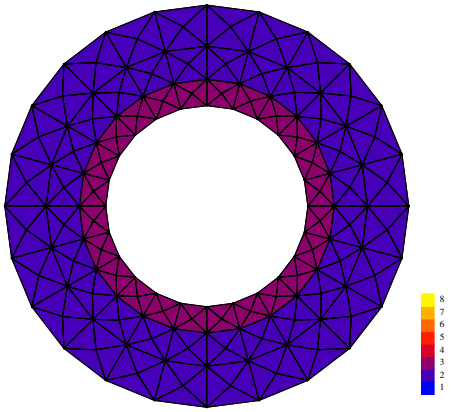

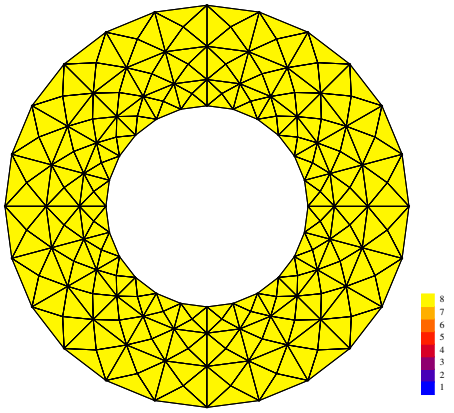

Fig. 4 Refined meshes: step 2 (*left*) and 8 (*right*)

elements in all triangles are shown in Fig. 3. The source term in (1) is $f = 1$. The exact solution expressed in polar coordinates is

$$u = \frac{(r_o^2 - r^2)\ln(r/r_i) - (r^2 - r_i^2)\ln(r_o/r)}{4\ln(r_o/r_i)}.$$

In this numerical example, the control parameters appearing in the algorithm have been chosen as follows: $\theta = \sqrt{0.5}$, $\gamma_h = 12$, $\gamma_p = 0.4$ and $\gamma_n = 3$. After four steps, the hp-scheme reaches the asymptotic behavior producing meshes with the same degree of polynomial p in all triangles. Thereafter, the adaptive algorithm only performs uniform p-refinement. Hence, the hp-version degenerates to the p-version, as expected in this example with regular solution. Figure 4 shows the meshes obtained with the adaptive hp-algorithm corresponding to step 2 and 8 of the refinement procedure.

It has been shown in Guo and Babuška (1986a,b) that a proper combination of h and p refinement, for such regular cases, allow us to obtain a rate of convergence

$$|e|_{H^1(\Omega)} \leq C\mathrm{e}^{-\alpha\sqrt{N}},$$

where N is the number of degrees of freedom in the finite element approximation (see Eq. (3.2) in Guo and Babuška 1986b). Figure 5 exhibits a plot of $\log|e|_{H^1(\Omega)}$ and $\log\eta_\Omega$ versus

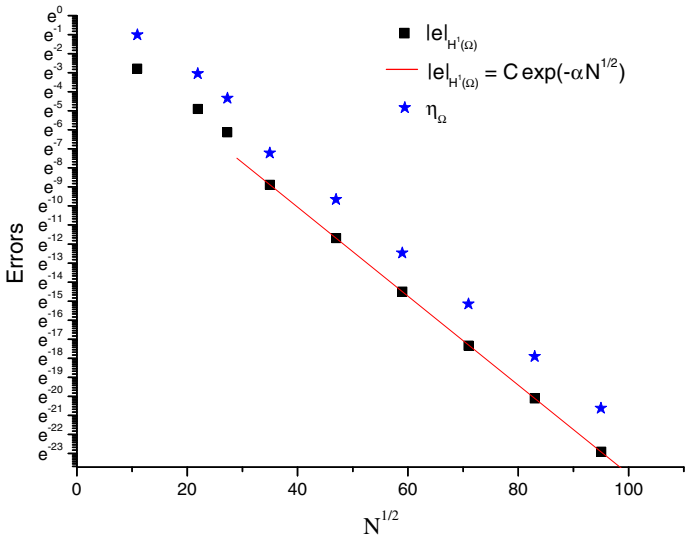

Fig. 5 Annular domain. Error and estimated error curves

Table 2 Concentric cylindrical tubes

Step	N	eff
0	120	0.16916
1	480	0.15547
2	744	0.16628
3	1, 224	0.18794
4	2, 208	0.13197
5	3, 480	0.13324
6	5, 040	0.11319
7	6, 888	0.10988
8	9, 024	0.10155

Effectivity indices

$\sqrt{N}$, which shows that both the error $|e|_{H^1(\Omega)}$ and the estimated error η_Ω attains such an exponential rate with $\alpha = 0.23$.

Since in this test, we know the analytical solution, we have used it to compute the so called *effectivity indices*:

$$\text{eff} := \frac{|e|_{H^1(\Omega)}}{\eta_\Omega}.$$

We report in Table 2 these indices at all steps. The table also includes the total number of degrees of freedom N for each step. It can be seen from this table that the effectivity indices remain bounded above and below throughout the refinement process.

We now proceed to solve the same problem using standard triangular elements with straight edges. The domain Ω is approximated by a polygonal domain Ω_h, and the presence of curved boundaries causes now a domain approximation error $(\Omega \setminus \Omega_h) \cup (\Omega_h \setminus \Omega)$ which we have not taken into account in the analysis. In this case, we have modified the adaptive algorithm as follows: when a new vertex appears on the straight edges approximating a curved boundary,

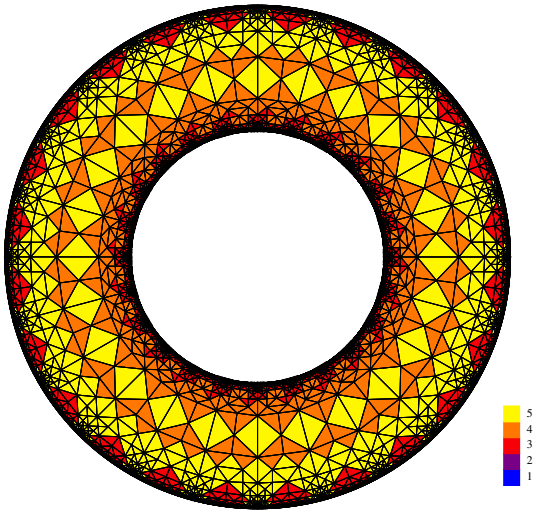

Fig. 6 Approximate annular domain: refined mesh, step 10

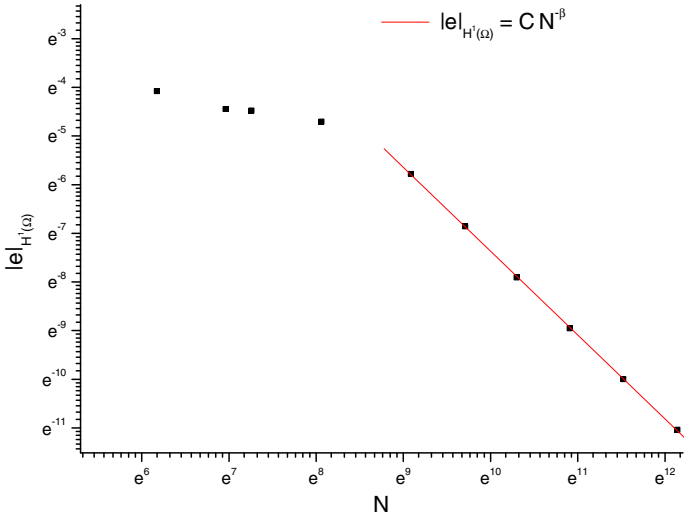

Fig. 7 Approximate annular domain: error curve

it was moved radially to the boundary. Note that the resulting family of meshes is not nested and, consequently, the error might increase.

Figure 6 shows the mesh and the distribution of degrees of polynomials obtained with the adaptive *hp*-algorithm corresponding to step 10 of the refinement procedure. We can see that the algorithm produces a large number of degrees of freedom that are spent approximating both boundaries. This does not occur when curved elements are used because the *h*-refinement is unnecessary in that case.

The appearance of this extra *h*-densification when noncurvilinear elements are used, causes a deterioration of the rate of convergence, which now is algebraic instead of exponential. Figure 7 exhibits this fact showing that the order of convergence obtained is

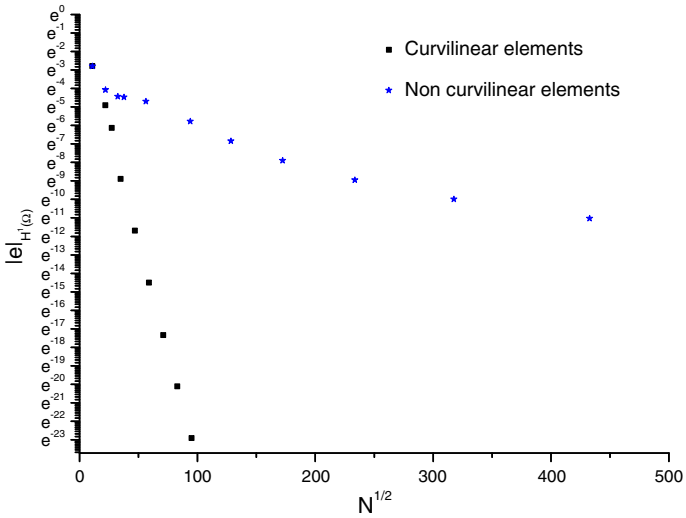

Fig. 8 Annulus domain: comparison of convergences

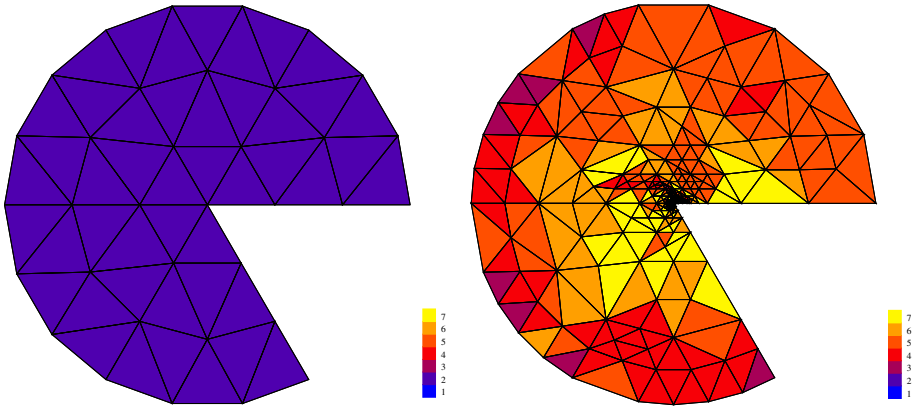

Fig. 9 Domain and initial mesh (*left*) and refined mesh: step 40 (*right*)

$$|e|_{H^1(\Omega)} \leq CN^{-\beta},$$

with $\beta = 1.72$.

Finally, Fig. 8 presents both rates of convergence in the same scale. This figure clearly indicates the performance improvement of the algorithm achieved using curvilinear elements.

5.2 Test 2: Pacman-shaped domain

In this second test, we have considered a Pacman-shaped domain centered in the origin with radius $r = 1$ and interior angle at the origin equal to $\frac{5}{3}\pi$. The domain and the initial mesh with quadratic finite elements in all triangles are shown in Fig. 9 (left). The initial mesh has 75 degrees of freedom.

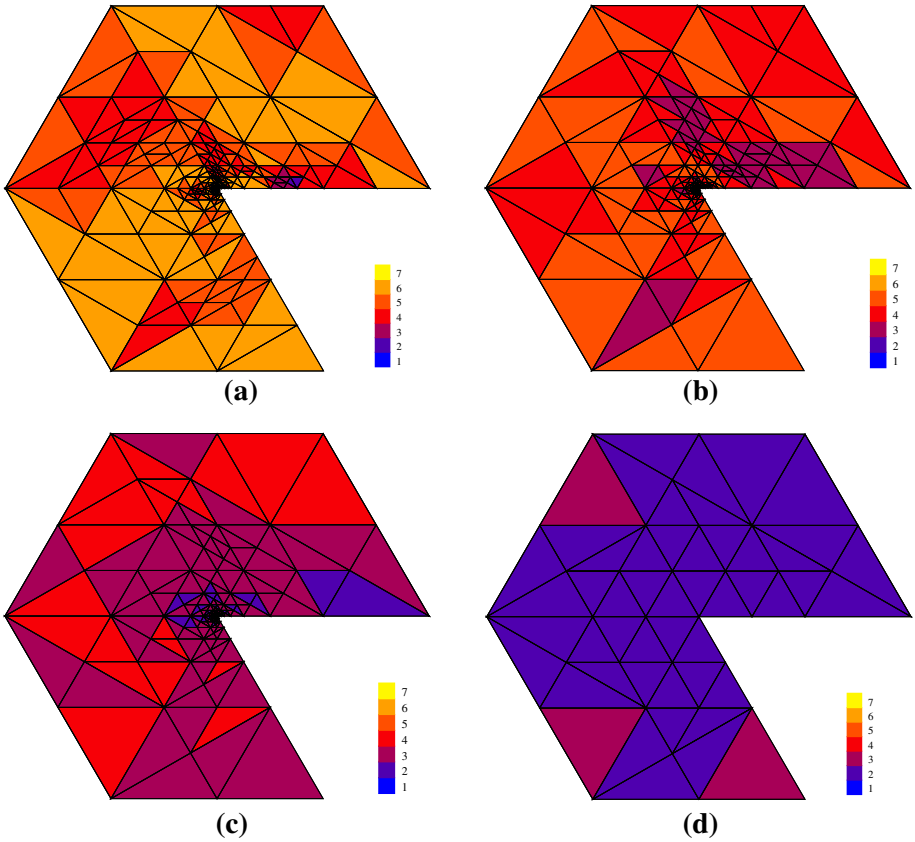

Fig. 10 Successive zooms at the vertex of the refined mesh at step 40

The source term in (1) and the corresponding exact solution in polar coordinates are $f = 1.6\, r^{-0.7} \sin(0.3\,\theta)$ and

$$u = r^{0.3}\,(1 - r)\sin(0.3\,\theta).$$

The control parameters appearing in the algorithm have been chosen as follows: $\theta = \sqrt{0.7}$, $\gamma_h = 20$, $\gamma_p = 0.4$ and $\gamma_n = 3$. Figure 9 (right) shows the mesh obtained with the adaptive hp-algorithm corresponding to step 40 of the refinement procedure. This final mesh has 20998 degrees of freedom.

The behavior of the adaptive algorithm in the neighborhood of the singularity can be appreciated from Fig. 10. This figure shows a sequence of zooms of the mesh at step 40 around the origin (the singular points). Zooms 10a–c and d enlarges the original mesh 10^3, 10^6, 10^9 and 10^{12} times, respectively. We observe the typical hp adaptive behavior: the closer to the singularity, the more dominant the h-refinement is, and in the elements nearest the singularity, there is no p-refinement at all. On the other hand, we see in Fig. 9 (right) that in the elements with edges lying on the curved boundary, the algorithm generates elements with high p-enrichment, and almost no h-refinement.

In this case, we are dealing with a singular solution. With an appropriate hp-refinement strategy, an exponential rate of convergence can still be achieved, but slightly lower than

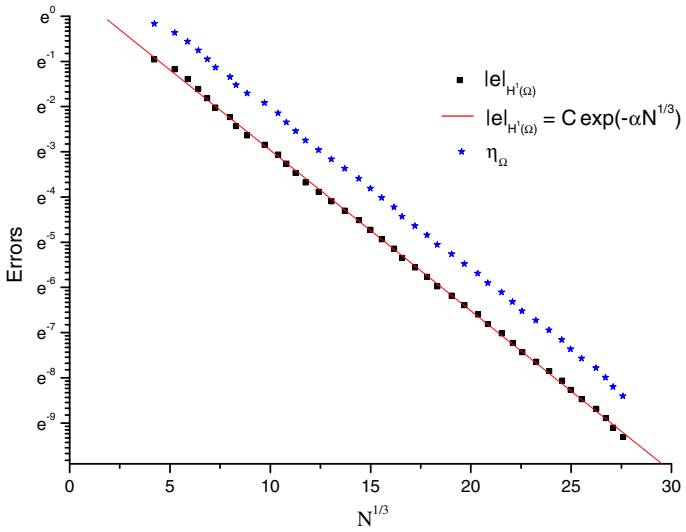

Fig. 11 Pacman-shaped domain. Error and estimated error curves

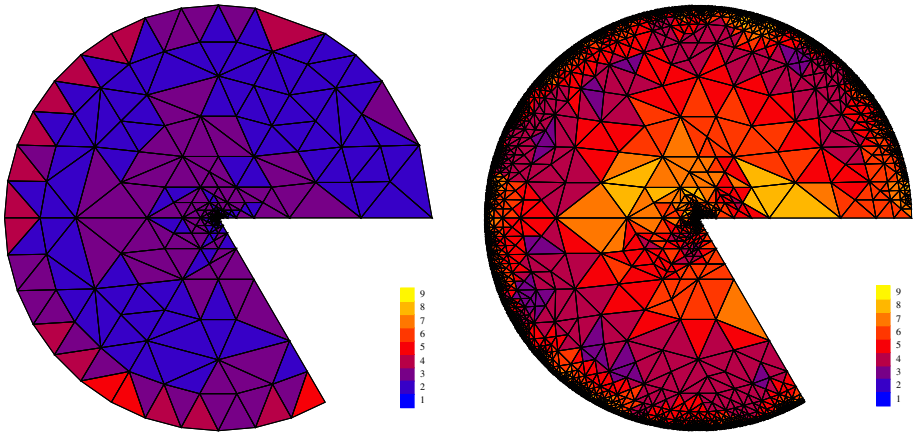

Fig. 12 Refined meshes: step 12 (*left*) and step 40 (*right*)

that obtained for the regular case (Guo and Babuška 1986a,b). This occurs because now the exponent is proportional to $\sqrt[3]{N}$ instead of $\sqrt{N}$. More precisely, (see Eq. (2.22) in Guo and Babuška 1986b)

$$|e|_{H^1(\Omega)} \leq C\mathrm{e}^{-\alpha\sqrt[3]{N}}. \tag{33}$$

Figure 11 exhibits a plot of $\log|e|_{H^1(\Omega)}$ and $\log\eta_\Omega$ versus $\sqrt[3]{N}$, which shows that both the error $|e|_{H^1(\Omega)}$ and the estimated error η_Ω attains such an exponential rate with $\alpha = 0.355$.

Similarly to the previous test, we now proceed to solve the same problem using standard triangular elements with straight edges. As we explained above, the new vertices, which appear on the straight edges approximating a curved boundary due to the h-refinement, will be displaced radially to the circular boundary. We start the adaptive procedure using a

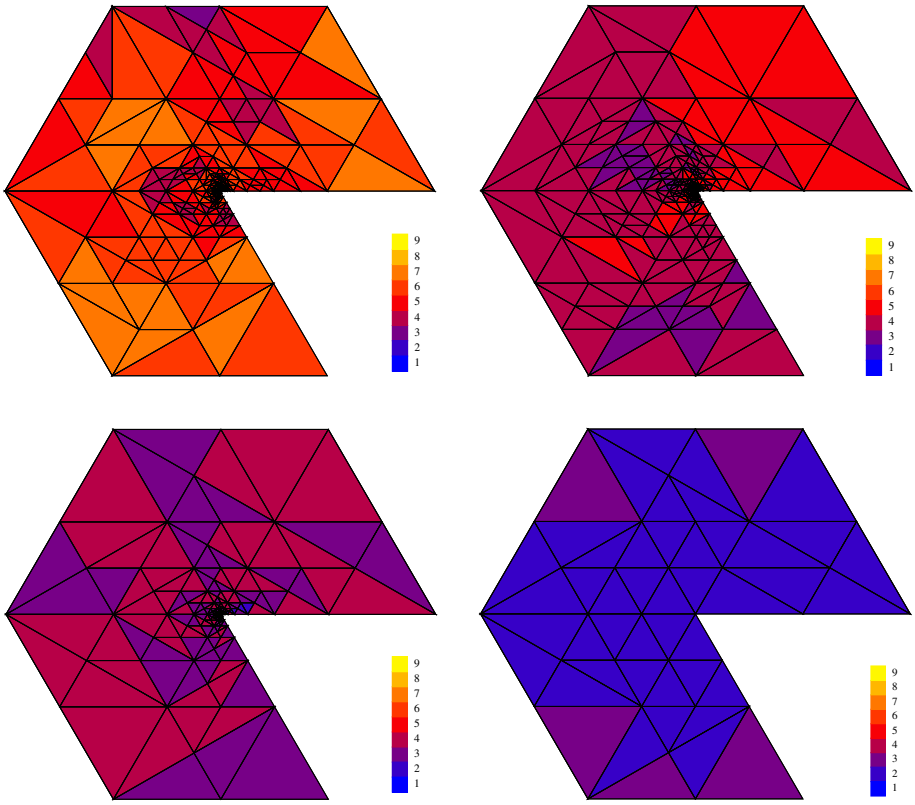

Fig. 13 Successive zooms at the vertex of the refined mesh at step 40

mesh similar to that in Fig. 9 (left) with the curved elements replaced by standard quadratic triangles.

In Fig. 12, the meshes obtained in steps 12 (left) and 40 (right) of the adaptive process are presented. Figure 13 presents the zooms analogous to those included in the case of curved elements, showing that the behavior of the algorithm near the reentrant vertex is qualitatively the same as before. However, Fig. 12 (right) shows the emergence of a strong h-refinement in the proximity of the circular boundary.

The algorithm is designed not only to reduce the global error, but also to obtain an equidistribution of local errors. In this case, the singularity in the origin is too strong and therefore, the new degrees of freedom added in the first steps concentrate in the neighborhood of the reentrant vertex. This fact is illustrated in Fig. 12 (left), which shows that the h-refinement is still insignificant near the circular boundary at step 12. From this step, the error indicators of the elements in the proximity of the origin and the ones near the circular boundary become comparable and the algorithm begins to refine in both places simultaneously.

Once again, the h-densification near the circular boundary turns the exponential decay of error (33) into the algebraic rate of convergence

$$|e|_{H^1(\Omega)} \leq CN^{-\beta},$$

with $\beta = 1.413$. This experimental fact is showed in Fig. 14.

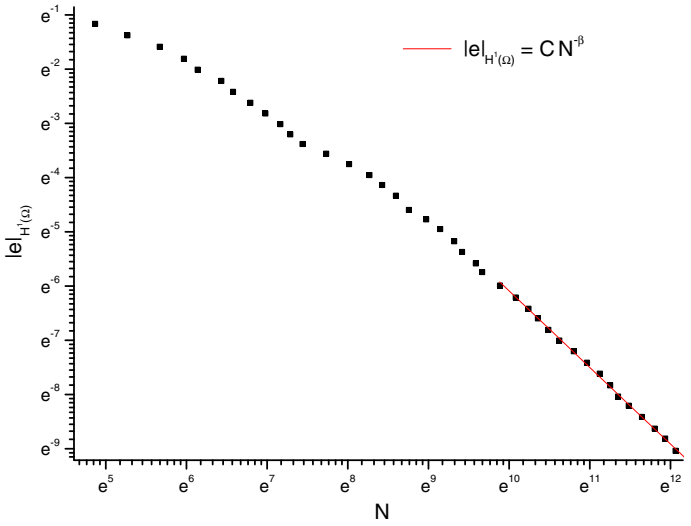

Fig. 14 Approximate pacman-shaped domain: error curve

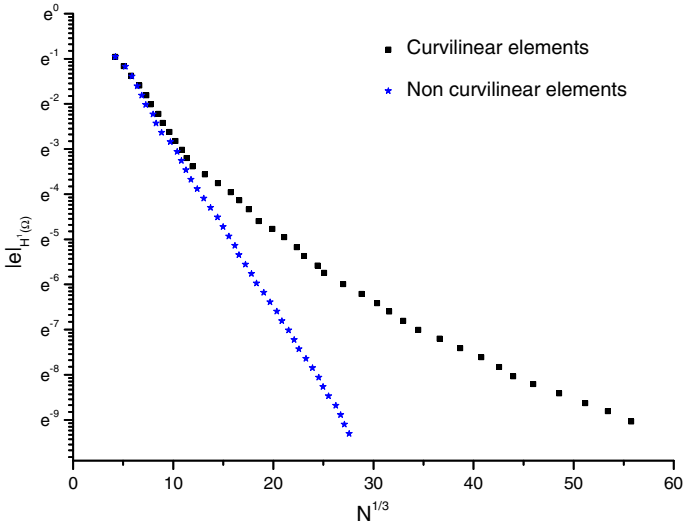

Fig. 15 Pacman-shaped domain: comparison of convergences

In Fig. 15, we compare both rates of convergence including a graphic analogous to that presented in Fig. 8. As before, we can see the performance improvement of the algorithm, when curvilinear elements are used. However, unlike what happens in regular case, both convergence curves have an overlapping zone during the first steps of the adaptive process. The reason of this was explained above: the presence of the strong singularity causes a concentration of degrees of freedom near the origin until the equidistribution of local error is achieved around step 12.

5.3 Test 3: Torsional stress in a splined shaft

Curved side splined shafts are common linkage components in key mechanical systems. The cross sections of such shafts present reentrant vertices, which become stress concentration points when the member is subjected to torsional loads.

The well-known theory by Saint-Venant poses the following problem to obtain the stress state of a noncircular shaft subjected to a torque M_T: find a function $u \in H_0^1(\Omega)$ such that $-\Delta u = 1$ and compute the corresponding stress components

$$\sigma_{13} = -\frac{M_T}{2k}\frac{\partial u}{\partial y} \qquad \text{and} \qquad \sigma_{23} = \frac{M_T}{2k}\frac{\partial u}{\partial x},$$

where $k = |u|^2_{1,\Omega}$. The angle of twist of the shaft per unit length θ_1 can be computed as

$$\theta_1 = \frac{M_T}{4Gk}, \tag{34}$$

where G is the shear modulus.

In this example, we consider a cylindrical shaft with six equidistributed teeth, whose cross section Ω is shown in Fig. 16 (left). The inner radius of the shaft is $r_i = 1$, and the outer radius is $r_o = 1.125$. Figure 16 (left) also exhibits the first triangulation of Ω, where curved element is used in triangles with at least one edge lying on the boundary $\partial\Omega$. The adaptive process starts with quadratic elements in all triangles and 792 degrees of freedom. Figure 16 (right) exhibits the refined mesh after 20 adapted steps. The final mesh has 122898 degrees of freedom, and the highest polynomial degree achieved is 7.

The behavior of the hp-adaptive processes is analogous to that described for the previous examples: h-refinement near the singularities and gradually increasing p-enrichment away from them. Exponential order of convergence is also achieved in this case for the error estimator η as a function of $\sqrt[3]{N}$, where N is the number of degrees of freedom. Figure 17 (left) sketches the torsion stress field shape $(\sigma_{13}, \sigma_{23})$. The norm of the stress varies from zero in the center of the shaft to infinity at the reentrant vertices. In order to visualize the stress distribution pattern, we have truncated the range setting the top of the scale to $M_T/2k$. This value corresponds to approximately 1.7 times the maximum torsional stress $2M_T/\pi$ of a circular shaft of radius 1 subjected to the same twisting moment M_T. The magnitude $\|(\sigma_{13}, \sigma_{23})\|/(M_T/2k)$ of this field is presented in Fig. 17 (right), which shows that the

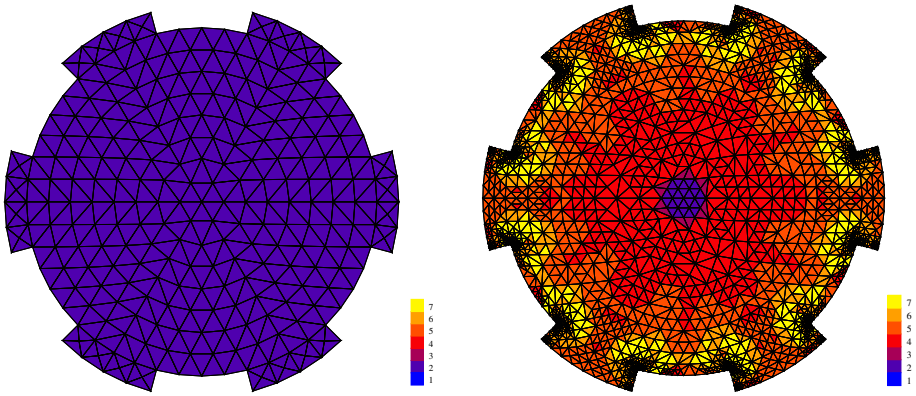

Fig. 16 Splined shaft, initial mesh (*left*) and refined mesh: step 20 (*right*)

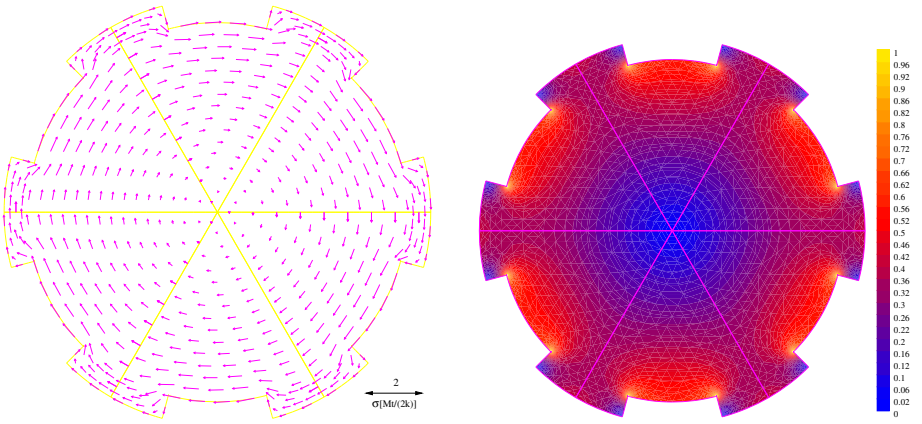

Fig. 17 Torsion stress field (*left*) and stress concentration zones (*right*)

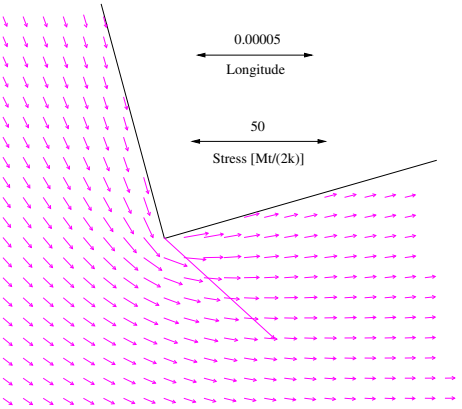

Fig. 18 Zoom of stress concentration zones

stresses are relatively small in most of the cross section. The stress concentration zones are strongly localized very close to the reentrant vertices. To illustrate in more detail the shape of the stress field in those areas, we have included Fig. 18, which shows a zoom of a singularity. Note that the tension is about 50 times higher than the top of the scale of the previous graph at the mesh node closest to the vertex. This fact shows the need for an efficient adaptive algorithm to accurately compute the stress distribution in this kind of practical problems.

Finally, we obtained $k = 0,4562580275023$. Thus, from (34), the torsional stiffness of the shaft $C := M_T/\theta_1$ results $C = 0,893111\, G\, I_p$, where $I_p = \int_\Omega r^2 d\Omega = 2,043454157$ is the polar moment of inertia of the cross section. That is, the torsional stiffness of the splined shaft is about 11 % lower than the one of a circular shaft with the same polar moment of inertia.

Acknowledgments This work was partially supported by ANPCyT under grant PICT 2010-01675. The first author was partially supported by ANPCyT under grant PICT-2007-00910 and by Universidad de Buenos Aires under grant 20020100100143. The first and second authors are members of CONICET, Argentina. The authors thank Dr. Mariano Cantero for helpful discussions concerning this work.

References

Ainsworth M, Senior B (1997) Aspects of an adaptive *hp* finite element method: adaptive strategy, conforming approximation and efficient solvers. Comput Methods Appl Mech Eng 150:65–87

Ainsworth M, Senior B (1998) An adaptive refinement strategy for *hp*-finite element computations. Appl Numer Math 26:165–178

Armentano MG, Padra C, Rodriguez R, Scheble M (2011) An hp finite element adaptive scheme to solve the Laplace model for fluid-solid vibrations. Comput Methods Appl Mech Eng 200(1–4):178–188

Armentano MG, Padra C, Rodriguez R, Scheble M (2012) An hp finite element adaptive method to compute the vibration modes of a fluid-solid coupled system, CMES. Comput Model Eng Sci 84(4):359–382

Azaiez M, Deville MO, Gruber R, Mund EH (2008) A new *hp* method for the -grad(div) operator in non-Cartesian geometries. Appl Numer Math 58:985–998

Babuška I, Suri M (1994) The P and H-P versions of the finite element method. Basci Princ Prop SIAM Rev 36:578–632

Babuška I, Suri M (1987) The *h*-*p* version of the finite element method with quasiuniform meshes. RAIRO Modél Math Anal Numér 21:199–238

Boffi D, Costabel M, Dauge M, Demkowicz L (2006) Discrete compactness for the *hp* version of rectangular edge finite elements SIAM. J Numer Anal 44:979–1004

Ciarlet PG (1978) The finite element method for elliptic problems, North Holland, Amsterdam

Ciarlet PG, Raviart PA (1972) Interpolation theory over curved elements with applications to finite element methods. Comput Methods Appl Mech Eng 1:217–249

Demkowicz L (2007) Computing with *hp*-adaptive finite elements, Vol. 1. One and two dimensional elliptic and Maxwell problems. Chapman & Hall/CRC, Boca Raton

Demkowicz L, Kurtz J, Pardo D, Paszyński M, Rachowicz W, Zdunek A (2008) Computing with *hp*-finite elements. Vol. 2. Frontiers: three-dimensional elliptic and maxwell problems with applications. Chapman & Hall/CRC, Boca Raton

Dorfler W, Heuveline V (2007) Convergence of an adaptive hp finite element strategy in one space dimension. Appl Numer Math 57:1108–1124

García-Castillo LE, Pardo D, Gómez-Revuelto I, Demkowicz LF (2007) A two-dimensional self-adaptive *hp* finite element method for the characterization of waveguide discontinuities. Part I: Energy-norm based automatic *hp*-adaptivity. Comput Methods Appl Mech Eng 196:4823–4852

Girault V, Raviart PA (1986) Finite element methods for Navier–Stokes equations. Springer, Germany, Berlin

Grisvard P (1985) Elliptic problems in nonsmooth domain. Pitman, Boston

Guo BQ, Babuška I (1986) The h-p-version of the finite element method. Part 1. Comput Mech 1:21–41

Guo BQ, Babuška I (1986) The h-p-version of the finite element method. Part 1. Comput Mech 1:203–226

Melenk JM (2005) *hp*-interpolation of nonsmooth functions and an application to *hp*-a posteriori error estimation. SIAM J Numer Anal 43(1):127–155

Melenk JM, Wohlmuth BI (2001) On residual-based a posteriori error estimation in hp-FEM. Adv Comput Math 15:311–331

Oden JT, Wu W, Ainsworth M (1995) Three-step *h*-*p* adaptive strategy for the incompressible Navier–Stokes equations, modeling, mesh generation, and adaptive numerical methods for partial differential equations. IMA Math Appl 75:347–366

Oden JT, Demkowicz L, Rachowicz W, Westermann TA (1989) Toward a universal *hp* adaptive finite element strategy, part 2. A posteriori error estimation. Comput Methods Appl Mech Eng 77:113–180

Oden JT, Patra A, Feng YS (1992) An *hp* adaptive strategy. In: Noor AK (ed) adaptive, multilevel and hierarchical computational strategies, AMD vol. 157, pp 23–46. ASME Publications

Pardo D, García-Castillo LE, Demkowicz LF, Torres-Verdín C (2007) A two-dimensional self-adaptive *hp* finite element method for the characterization of waveguide discontinuities. Part II: Goal-oriented *hp*-adaptivity. Comput Methods Appl Mech Eng 196:4811–4822

Scott R (1975) Interpolated boundary conditions in the finite element method. SIAM J Numer Anal 12:404–427

Schwab Ch (1998) p- and hp- finite element methods, Theory and applications in solid and fluid mechanics (Numerical Mathematics and Scientific Computation). Oxford University Press

Tarancon JE, Fuenmayor FJ, Baeza L (2005) An a posteriori error estimator for the *p*- and *hp*-versions of the finite element method. Intern J Numer Methods Eng 62:1–18

Verfürth R (1996) A review of a posteriori error estimation and adaptive mesh-refinement techniques. Wiley & Teubner, New York

Zlâmal M (1973) Curved elements in the finite element method I. SIAM J Numer Anal 10(1):229–240